

C.P. No. 660

C.P. No. 660



MINISTRY OF AVIATION

AERONAUTICAL RESEARCH COUNCIL

CURRENT PAPERS

Room Temperature Instability and Fraction in
Rotating Discs and Correlation with
Bi-axial Tensile Test Data

By

N.E. Waldren and D.E. Ward

LONDON: HER MAJESTY'S STATIONERY OFFICE

1963

SIX SHILLINGS NET

Room temperature instability and fraction in
rotating discs and correlation with
bi-axial tensile test data

- by -

N. I. Waldren and D. E. Ward

SUMMARY

The room temperature burst strength and ductility of model discs in a typical ferritic turbine disc material (Rex 535) has been examined.

Discs from vacuum melted bar exhibited remarkably consistent properties. The discs burst when the average tangential stress exceeded the ultimate tensile strength of the material by as much as 7 per cent. A detailed analysis of the more ductile discs supports the use of the distortion energy (Von Mises) and deformation (Hencky) theories for predicting disc instability. In the case of the less ductile discs, results from tubes in bi-axial tension confirm failure when this occurs before the point of instability.

CONTENTS

| | <u>Page</u> |
|---|-------------|
| 1.0 Introduction | 4 |
| 2.0 General results of disc burst tests | 4 |
| 3.0 Detailed analysis of disc burst results | 4 |
| 3.1 Tensile test data (uni-axial) | 5 |
| 3.2 Average tangential stress and measured strain | 6 |
| 3.3 Estimated bi-axial stress | 7 |
| 3.4 Condition for disc instability | 9 |
| 3.5 Tensile test data (bi-axial) | 10 |
| 4.0 Conclusions | 11 |
| Notation | 13 |
| References | 14 |
| Detachable Abstract Cards | |

TABLES

| <u>No.</u> | <u>Title</u> | |
|------------|---|----|
| I | Rex 535 model disc burst results (bar) | 15 |
| II | Rex 535 model disc burst results (forged) | 16 |

ILLUSTRATIONS

| <u>Fig. No.</u> | <u>Title</u> |
|-----------------|--|
| 1 | Details of model discs and test rig (full scale) |
| 2 | Comparison between burst strength of air and vacuum melt (bar and forged) discs in Rex 535 steel |
| 3(a) | Stress/strain data for Rex 535 vacuum melt bar |
| 3(b) | Log true stress/log natural strain data for Rex 535 vacuum melt bar |
| 4 | Plastic distortion in discs related to bore tangential strain |
| 5 | Burst strength and ductility of discs from Rex 535 vacuum melt bar |

ILLUSTRATIONS (cont'd)

| <u>Fig. No.</u> | <u>Title</u> |
|-----------------|---|
| 6 | Principal plastic strains in discs at burst |
| 7 | Distribution of radial/tangential stress ratio in discs at burst |
| 8(a) | Distribution of tangential stress/strain in discs at burst (V.P.N. 336) |
| 8(b) | Distribution of tangential stress/strain in discs at burst (V.P.N. 364) |
| 9 | Distribution of stress in discs at burst (V.P.N. 336) |
| 10 | The influence of geometry on instability |
| 11 | Disc and tube nominal burst results in relation to instability |
| 12 | Cracks around bore of disc No. 3367 after 12 per cent bore tangential strain (95,800 rev/min) |
| 13 | Proposed method of assessing disc strength from tube data |

1.0 Introduction

This Memorandum describes the use of model disc burst results as a means of evaluating, at room temperature, a typical ferritic turbine disc material for an aircraft gas turbine engine.

Initially the work was aimed at assessing the influence of vacuum melting and forging on Firth Vickers Rex 535 turbine disc steel in co-operation with Rolls-Royce Ltd. but a more detailed analysis has resulted in the course of the current turbine disc investigation at the N.G.T.E.¹.

Simple model discs in both air and vacuum melted versions of the steel were manufactured by Rolls-Royce Ltd. and spun to burst, at room temperature, in the small spinning rig at N.G.T.E., Pyestock. Some discs were sliced from large diameter bar while others were forged up from small diameter billets being subjected to the equivalent forging work of a full scale engine disc. Heat treatment was also varied to produce discs in two conditions of strength and ductility identifiable by high and low values of hardness.

2.0 General results of disc burst tests

The dimensions of the model discs used in the evaluation are given in Figure 1. All discs were ground flat and bored at the centre and, in a small number of cases, deep notches were broached in the bore to simulate severe flaws or stress raisers.

The general burst results are listed in Tables I and II. In some cases it was not possible to reach burst conditions, even after many attempts, due to failure of the flexible drive shaft. The maximum conditions attained by these discs are therefore identified by brackets.

The average tangential stress, calculated from the speed, has been included as a measure of disc strength and the reduction in bore axial thickness as a measure of ductility.

The influence of the various material conditions on the model discs can be seen in Figure 2 in which the maximum rotational speed of each disc has been plotted against hardness. Dotted lines indicate the general trend of disc strength. Discs sliced from vacuum melted bar exhibit remarkably consistent properties, whereas discs from the air melted bar show considerable scatter. The influence of forging is not clear due to insufficient disc burst data. It might be concluded, however, that forging has improved the air melted bar but has introduced more scatter into the vacuum melt bar. Notched bored discs exhibited higher strength at the lower end of the hardness range where greater ductility might be expected.

3.0 Detailed analysis of disc burst results

The uniform properties exhibited by the vacuum melted bar encourages an attempt to correlate the stress/strain behaviour and the burst strength of the discs in these two batches with simple tensile data. In addition to examining the fit of the plastic deformation theory used in this correlation it would be of interest to study the instability condition for the discs together with the results obtained from bi-axially stressed test pieces either of which may identify the cause of failure.

3.1 Tensile test data (uni-axial)

The simple tensile stress/strain data for the vacuum melted bar in the two heat-treated conditions are given in Figure 3(a). The test pieces were located tangentially at bore and rim in the sample blank representing each batch and the following nominal results confirm almost uniform properties throughout:-

| Tensile test data (uni-axial) | Rex 535 Vacuum melted bar | | | |
|--|------------------------------|------|------|------|
| | Bore | Rim | Bore | Rim |
| 0.1% proof stress, tons/sq in. | 54.5 | 56.0 | 59.9 | 61.6 |
| | 56.1 | 56.8 | 59.9 | 60.6 |
| Ultimate tensile strength, tons/sq in. | 65.6 | 67.4 | 77.0 | 77.0 |
| | 66.2 | 67.3 | 77.7 | 77.7 |
| Fracture, R of A, % | 33 | 28 | 57 | 51 |
| | 31 | 16 | 40 | 51 |
| Fracture, elong., % | 15 | 13 | 14 | 17.5 |
| | 14 | 19 | 14 | 16 |
| Hardness, V.P.N. | 336 | | 364 | |

True stress/strain has been obtained from the test piece data in the following manner:-

$$\text{Nominal stress} = \sigma' = \frac{\text{load}}{\text{original area}}$$

$$\text{Nominal strain} = \epsilon'$$

$$\text{where } 1 + \epsilon' = \frac{\text{original area}}{\text{actual area}}$$

$$\text{True stress} = \sigma = \sigma'(1 + \epsilon')$$

$$\text{Natural strain} = \epsilon = \log_e(1 + \epsilon')$$

The true stress/strain relation for a strain hardening material in simple tension may be closely approximated by the following exponential relation:-

$$\sigma = K\epsilon^n$$

where σ = true stress
 ϵ = natural strain
K = strength coefficient
n = strain hardening exponent

The point of instability (maximum load) in this exponential relation occurs when the strain, $\epsilon = n$. This can be seen in Figure 3(b) in which true stress/strain has been plotted on a log.log basis, n being the slope of the line.

3.2 Average tangential stress and measured strain

The average of the tangential stress in a rotating thin disc may be calculated directly from the speed using the following formula based on the original dimensions of the disc:-

$$\begin{aligned} \text{Nom. av. tan. stress} &= \frac{\rho}{g} \cdot \omega^2 \cdot \frac{1}{3} \cdot \frac{r_1^3 - r_2^3}{r_1 - r_2} \\ &= 75.9 \times \left(\frac{\text{rev/min}}{100,000} \right)^2 \text{ tons/sq in.} \end{aligned}$$

where ω = angular velocity - radians/s
 ρ = density = 0.28 lb/cu in. for steel
 g = 32.2 ft/s²
 r_1 = rim radius = 2.4 in.
 r_2 = bore radius = 0.25 in.

At this stage in the analysis it is important to note that all discs from the vacuum melted bar, burst when the nominal average tangential stress recorded in Table I exceeded the Ultimate Tensile Strength of the material in Section 3.1 by 6 per cent for the lower hardness range (V.P.N. 336) and 7 per cent for the higher hardness range (V.P.N. 364).

As the speed of the disc increases from zero to the point of burst local high elastic stresses first enter the plastic range and redistribution of stress takes place. The whole disc then becomes plastic and a permanent increase in diameter and a reduction in thickness occur. In the plastic range, changes in disc shape may be considerable and a correction must therefore be applied to the nominal value of the average tangential stress to allow for these changes.

The stress in the bore of a rotating thin disc is uni-axial. The bore tangential strain should therefore bear a linear relationship to the change in axial thickness at the bore in a similar manner to the tensile test piece. This is confirmed by the experimental data plotted in Figure 4. Bore tangential strain may therefore be obtained from the maximum axial thickness of the burst fragments.

For convenience the plastic deformation throughout the disc may be related to the bore strain and a correction applied to the average tangential stress in the following manner:-

$$\sigma_1 = \sigma_1' (1 + 0.34 \epsilon_1')$$

where ϵ_1' = bore tangential strain

σ_1' = nominal average tangential stress

σ_1 = true average tangential stress

and the value 0.34 has been obtained experimentally.

In order to compare the strength and ductility of the discs in each batch the true average tangential stress at burst has been plotted against the bore tangential strain for each disc in Figure 5. The dotted line indicates the simple tensile properties for the batch. The reason why the average tangential stress lies close to this dotted line will be seen later. Discs Nos. 3368 and 3369 (V.P.N. 338 and 334 respectively) have been chosen to represent the range for the correlation with the tensile test data (V.P.N. 336).

The axial strain, ϵ_3 , at burst for discs Nos. 3368 and 3369 has been plotted in Figure 6. From this the tangential strain, ϵ_1 , at bore and rim has been deduced assuming uni-axial conditions and an incompressible material, i.e. $\epsilon_1 + \epsilon_2 + \epsilon_3 = 0$ and $\epsilon_2 = \epsilon_3$. The distribution of radial and tangential strain has been carefully drawn in using as a guide the strain grid results of other discs of identical geometry.

3.3 Estimated bi-axial stress

Having established the distribution of the three principal strains in the disc it is now necessary to assume a relation between strain and stress to obtain the distribution of radial and tangential stress at burst.

The following equations for the "uni-axial equivalent" or significant stress and strain in a multi-axial stress system are based on distortion energy (Von Mises) theory^{2,3}.

$$\bar{\sigma} = \frac{\sqrt{2}}{2} \left[(\sigma_1 - \sigma_2)^2 + (\sigma_2 - \sigma_3)^2 + (\sigma_3 - \sigma_1)^2 \right]^{\frac{1}{2}}$$

$$\bar{\epsilon} = \frac{\sqrt{2}}{3} \left[(\epsilon_1 - \epsilon_2)^2 + (\epsilon_2 - \epsilon_3)^2 + (\epsilon_3 - \epsilon_1)^2 \right]^{\frac{1}{2}}$$

where σ_1 , σ_2 and σ_3 are the principal stresses and ϵ_1 , ϵ_2 and ϵ_3 the resulting principal strains. The constants $\frac{\sqrt{2}}{2}$ and $\frac{\sqrt{2}}{3}$ are so chosen that $\bar{\sigma} = \sigma_1$ and $\bar{\epsilon} = \epsilon_1$ for simple uni-axial tension.

In a thin rotating disc the tangential stress σ_1 is greater than the radial stress σ_2 and the axial stress σ_3 is assumed to be zero, i.e. $\sigma_1 \geq \sigma_2$ and $\sigma_3 = 0$.

The equation for stress therefore reduces to:-

$$\bar{\sigma} = (\sigma_1^2 - \sigma_1\sigma_2 + \sigma_2^2)^{\frac{1}{2}}$$

or

$$\bar{\sigma} = \sigma_1 (1 - x + x^2)^{\frac{1}{2}}$$

where x denotes the stress ratio σ_2/σ_1 .

The Hencky deformation theory relates the principal stresses and strains in a multi-axial stress system in the following equations:-

$$\epsilon_1 = \frac{\bar{\epsilon}}{\bar{\sigma}} \left[\sigma_1 - \frac{1}{2} (\sigma_2 + \sigma_3) \right]$$

$$\epsilon_2 = \frac{\bar{\epsilon}}{\bar{\sigma}} \left[\sigma_2 - \frac{1}{2} (\sigma_1 + \sigma_3) \right]$$

$$\epsilon_3 = \frac{\bar{\epsilon}}{\bar{\sigma}} \left[\sigma_3 - \frac{1}{2} (\sigma_1 + \sigma_2) \right]$$

These equations may be rewritten to produce the following relation between principal strain and stress ratio for the model discs:-

$$\frac{\bar{\epsilon}}{2(1-x+x^2)^{\frac{1}{2}}} = \frac{\epsilon_1}{2-x} = \frac{\epsilon_2}{2x-1} = \frac{-\epsilon_3}{1+x}$$

By introducing the measured plastic strain into this equation the distribution of radial/tangential stress ratio, at burst may be obtained. This has been plotted in Figure 7.

The maximum principal stress, σ_1 , in the thin disc will be in a tangential direction and in order to obtain the level of this stress at the point of burst it is now necessary to refer to stress/strain data obtained from the tensile test pieces and plotted in Figures 3(a) and 3(b). These uni-axial data form the basis for the curves of maximum principal stress/strain in Figure 8(a) calculated for various ratios of bi-axial stress. With the aid of the tangential strain and stress ratio plotted in Figures 6 and 7 the distribution of tangential stress/strain at the point of burst may now be drawn on the curves of Figure 8(a).

In Figure 9 the distribution of tangential stress obtained from the previous figure compares favourably with values of true average tangential stress for each disc and would confirm the stress/strain relationship used in the analysis.

3.4 Condition for disc instability

In order to understand the conditions for instability in the model discs it is best to examine first, a thin rotating ring, then a plain disc with a uniform distribution of equi-bi-axial stress. The models lie between these two extremes.

It may be assumed that the material in a thin rotating ring will be subjected to a single tangential stress and will therefore behave in a similar manner to a tensile test piece which has been bent into a full circle. In addition to the reduction of area that will occur with tangential strain, however, an increase in centrifugal loading due to the increase in the radius of the C.G. will also occur, both being linear to the tangential strain. The result will be a maximum in speed at a lower strain than at ultimate in simple tension. This may be expressed in the following manner:-

$$\text{Tangential stress, } \sigma_1 = \rho \omega^2 r^2$$

Differentiating and equating the rate of increase in angular velocity to zero we have

$$\frac{d\sigma_1}{\sigma_1} = 2 \frac{dr}{r} = 2\varepsilon_1$$

where ε_1 is the tangential strain.

Instability for a rotating thin ring therefore occurs at half the strain for instability in simple tension and at a tangential stress lower than the Ultimate Tensile Strength. This is shown graphically in Figure 10 using the stress/strain data of Figure 3(a) (V.P.N. 364).

Similarly a disc with both uniform stress and uniform stress ratio will reach instability at half the strain for that in simple tension. This latter stress condition can only be met by a solid, profiled disc with rim loading, the stress being uniform and equi-bi-axial. This also is shown in Figure 10 from which it will be observed that, in this case, the maximum stress is equal to the Ultimate Tensile Strength.

The model discs under consideration have non-uniform stress and varying stress ratio and the problem of instability is therefore more complex. For these discs, however, experimental data have indicated the following relation between the rate of increase in average tangential stress, σ_1 and the mean tangential strain, ε_1 :-

$$\sigma_1 = \sigma_1' (1 + 1.7 \varepsilon_1')$$

where ε_1' = mean tangential strain

= 0.2 x bore tangential strain (see Figure 6)

These data suggest that instability in the model discs should occur when the mean tangential strain reaches a value of $\frac{1}{1.7} \times$ the strain at instability in simple tension, i.e. $\epsilon_1'(\text{mean}) = \frac{0.062}{1.7} = 0.036$.

Discs in the lower hardness range (V.P.N. 336) do not appear to have reached the instability condition, the mean tangential strain at burst being less than 0.02. This is supported by the absence of necking in the burst fragments. However, discs in the higher hardness range (V.P.N. 364) would seem to be within the region of instability and one disc (No. 3366) did in fact burst on reducing speed. In this disc local necking occurred and mean tangential strain was very close to the expected value for instability (Figure 8(b)).

3.5 Tensile test data (bi-axial)

So far it has been possible to relate the stress/strain behaviour of the disc with simple tensile data and to locate, to a reasonable degree of accuracy, the point of instability for various disc geometries. The simple tensile test however does not indicate the ductility of a material when stressed by rotation and another form of test other than a spinning test would seem desirable.

In the previous section the stress/strain behaviour of the model discs was represented by the average tangential stress/strain. If it is assumed that the maximum radial/tangential stress ratio is significant then the disc stress/strain may be plotted in Figure 11 for an 0.7 stress ratio.

In order to produce a bi-axial tension of 0.7 stress ratio under more controlled conditions a number of tubes of disc material were subjected to combined internal hydraulic pressure and tension. An axial/tangential stress ratio of 0.7 was produced in the thin wall and the following nominal results obtained:-

| Tensile test data (bi-axial) | Rex 535 Vacuum melt bar | |
|---------------------------------------|----------------------------|------|
| | Bore | Bore |
| Axial/tangential stress ratio | 0.7 | 0.7 |
| Nominal max. tan. stress, tons/sq in. | 67.9 | 84.6 |
| Tan. strain (instab. 2.5%), -% | 1.0 | 2.1 |
| Hardness, V.P.N. | 336 | 364 |

The relation between tangential stress/strain for a stress ratio of 0.7 in the tube may be obtained in the following manner:-

$$\text{Nominal tangential stress } \sigma_1' = \frac{Pr}{t}$$

where P = internal hydraulic pressure

r = mean radius of tube wall

t = thickness of tube wall

$$\begin{aligned} \text{True tangential stress } \sigma_1 &= \sigma_1' \frac{(1 + \epsilon_1')}{(1 - \epsilon_2')} \\ &= \sigma_1'(1 + 2.3 \epsilon_1') \text{ approximately} \end{aligned}$$

$$\begin{array}{l} \text{where } \epsilon_1' = \text{tangential strain, } \frac{dr}{r} = +1.0 \\ \epsilon_2' = \text{radial strain, } \frac{dt}{t} = -1.3 \\ \epsilon_3' = \text{axial strain} = +0.3 \end{array} \left. \vphantom{\begin{array}{l} \epsilon_1' \\ \epsilon_2' \\ \epsilon_3' \end{array}} \right\} \begin{array}{l} \text{proportional strains} \\ \text{for 0.7 stress ratio} \end{array}$$

It is of interest to compare the results obtained from the tubes with those of the discs in Figure 11. The tangential strain is of particular significance.

Further confirmation that failure in the discs has been due to bi-axial tension is given in Figure 12 in which it is shown that cracking has been located some distance from the bore.

A method of assessing disc strength using the results of tubes in bi-axial tension is outlined in Figure 13. The calculation of disc strain is a laborious process and is best carried out on a computer. Fortunately, the stress ratio changes very little and this means that the ratio of the elastic stresses may be used as a close guide when selecting the appropriate stress ratio for the tubes.

The strain at instability in tubes subjected to internal pressure and tension is less than the strain at instability in thin, rotating discs. This feature may limit the use of the tubes but, nevertheless, the available range is of great value in assessing disc materials.

4.0 Conclusions

The following conclusions may be drawn from a general examination of the disc burst results.

1. Remarkably consistent properties and good strength were exhibited by discs from Rex 535 vacuum melt bar. Discs from air melt bar showed considerable scatter. The influence of forging is not clear due to insufficient disc burst data. It might be concluded, however, that forging has improved the air melt bar but has introduced more scatter into the vacuum melt bar.

2. Discs from Rex 535 vacuum melt bar, burst when the average of their tangential stress exceeded the Ultimate Tensile Strength of the material by as much as 7 per cent.

3. Discs and test pieces from the Rex 535 vacuum melt bar in the higher hardness range (V.P.N. 364) had higher strength and, contrary to expectation, slightly better ductility than those in the lower hardness range (V.P.N. 336). This may have been due to poor heat treatment in the latter case or is perhaps an inherent feature of this material.

The following additional conclusions may be drawn from a detailed examination of selected discs from the Rex 535 vacuum melt bar.

4. Failure in discs in the lower hardness range would seem to be due to limited ductility caused by bi-axial tension. This is supported by internal cracking in the discs some distance from the bore and is further supported by results from tubes in bi-axial tension. Similar failures occurred in discs in the higher hardness range but some discs in this range had sufficient ductility to allow instability to occur.

5. It would appear from the analysis that the distortion-energy (Von Mises) and deformation (Hencky) theories may be used with a reasonable degree of reliability in the plastic analysis of discs over the whole plastic range to the point of instability or burst.

6. The agreement between results from rotating model discs and tubes under combined hydraulic pressure and tension would confirm the value of the latter or other similar methods for evaluating disc materials.

NOTATION

| | | | |
|-------------------------------------|---|---|--|
| σ' | = | nominal stress | |
| ϵ' | = | nominal strain | |
| σ | = | true stress = $\sigma'(1 + \epsilon')$ | |
| ϵ | = | natural strain = $\log_e(1 + \epsilon')$ | |
| K | = | strength coefficient | } in the relation $\sigma = K\epsilon^n$ |
| n | = | strain hardening exponent | |
| σ_1 and ϵ_1 | = | true tangential stress and strain (Max principal) | |
| σ_2 and ϵ_2 | = | true radial stress and strain | |
| σ_3 and ϵ_3 | = | true axial stress and strain | |
| $\bar{\sigma}$ and $\bar{\epsilon}$ | = | significant or uni-axial equivalent stress and strain | |
| $x = \sigma_2/\sigma_1$ | = | radial/tangential stress ratio | |
| ω | = | angular velocity - radians/s | |
| ρ | = | density - lb/cu in. | |
| g | = | 32.2 ft/s ² | |
| r_1 | = | disc rim radius | |
| r_2 | = | disc bore radius | |
| r | = | radial station in disc or mean radius of tube wall | } in relation to tubes with internal hydraulic pressure |
| P | = | hydraulic pressure | |
| t | = | tube wall thickness | |

REFERENCES

| <u>No.</u> | <u>Author(s)</u> | <u>Title, etc.</u> |
|------------|-----------------------------|---|
| 1 | N. E. Waldron D. E. Ward | The experimental correlation of rotating disc burst strength with conventional material data. Part I - Room temperature burst tests on model discs with plain bores. Unpublished M.O.A. Report. |
| 2 | Geo. E. Dieter Jr. | Mechanical Metallurgy. McGraw-Hill, 1961. |
| 3 | P. B. Mellor | Plastic instability in tension. The Engineer, 25th March, 1960. (Technical Contribution Section) |

TABLE I

Rex 535 model disc burst results (bar)
(0.5 in. bore 4.8 in. o.d. 1.0 in. thick)

| Reference | Hardness V.P.N. | | Maximum speed rev/min | Nominal average tangential stress tons/sq in. | Maximum thickness at bore inches |
|---------------------------|--------------------|-----|-----------------------------|--|---|
| | Bore | Rim | | | |
| a. <u>Bar/air melt</u> | | | | | |
| 3354 | 375 | 373 | 99,210 | 74.7 | 0.977 |
| 3355 | 375 | 375 | 89,500 | 60.8 | 0.990 |
| 3356 | 387 | 387 | 98,000 | 72.9 | 0.981 |
| 3357 | 371 | 377 | 97,820 | 72.6 | 0.984 |
| 3358 | 364 | 366 | 97,040 | 72.0 | 0.984 |
| 3359 | 375 | 375 | 82,890 | 52.3 | 0.993 |
| 3377 | 358 | 357 | 96,350 | 70.4 | 0.985 |
| 3378 | 342 | 341 | 94,800 | 68.2 | 0.964 |
| 3379 | 327 | 326 | 95,090 | 68.6 | 0.981 |
| 3380 | 344 | 338 | 92,940 | 65.6 | 0.988 |
| 3381 | 331 | 331 | 88,560 | 59.5 | 0.990 |
| 3382 | 336 | 336 | (75,000) | flaws in bore | (0.98) |
| b. <u>Bar/vacuum melt</u> | | | | | |
| 3360 | 379 | 379 | (102,100) | 79.0 | 0.944 |
| 3361 | 371 | 371 | 104,400* | 82.9 | 0.928 |
| 3362 | 364 | 364 | 103,500 | 81.3 | 0.964 |
| 3363 | 366 | 360 | 102,660 | 79.8 | 0.969 |
| 3364 | 364 | 364 | | Cut for test pieces | |
| 3365 | 374 | 375 | 104,520* | 83.0 | 0.897 } local |
| 3366 | 361 | 383 | 104,820 [‡] | 83.2 | 0.924 } necking |
| 3367 | 314 | 319 | (95,800) [‡] | (69.7) | (0.944) |
| 3368 | 335 | 340 | 95,900 | 69.9 | 0.959 |
| 3369 | 334 | 334 | 95,380 | 69.0 | 0.972 |
| 3370 | 336 | 336 | 95,460 | 69.2 | 0.968 |
| 3371 | 336 | 345 | 95,590 | 69.5 | 0.961 |
| 3372 | 339 | 333 | | Cut for test pieces | |
| 3373 | 330 | 322 | 95,400 | 69.1 | 0.949 |

Figures in brackets are for discs not burst

*Burst at lower speed in subsequent test

[‡]Burst on reducing speed to 103,000 rev/min

[‡]Photomicrograph

TABLE II

Rex 535 model disc burst results (forged)
 (0.5 in. bore 4.8 in. o.d. 1.0 in. thick)

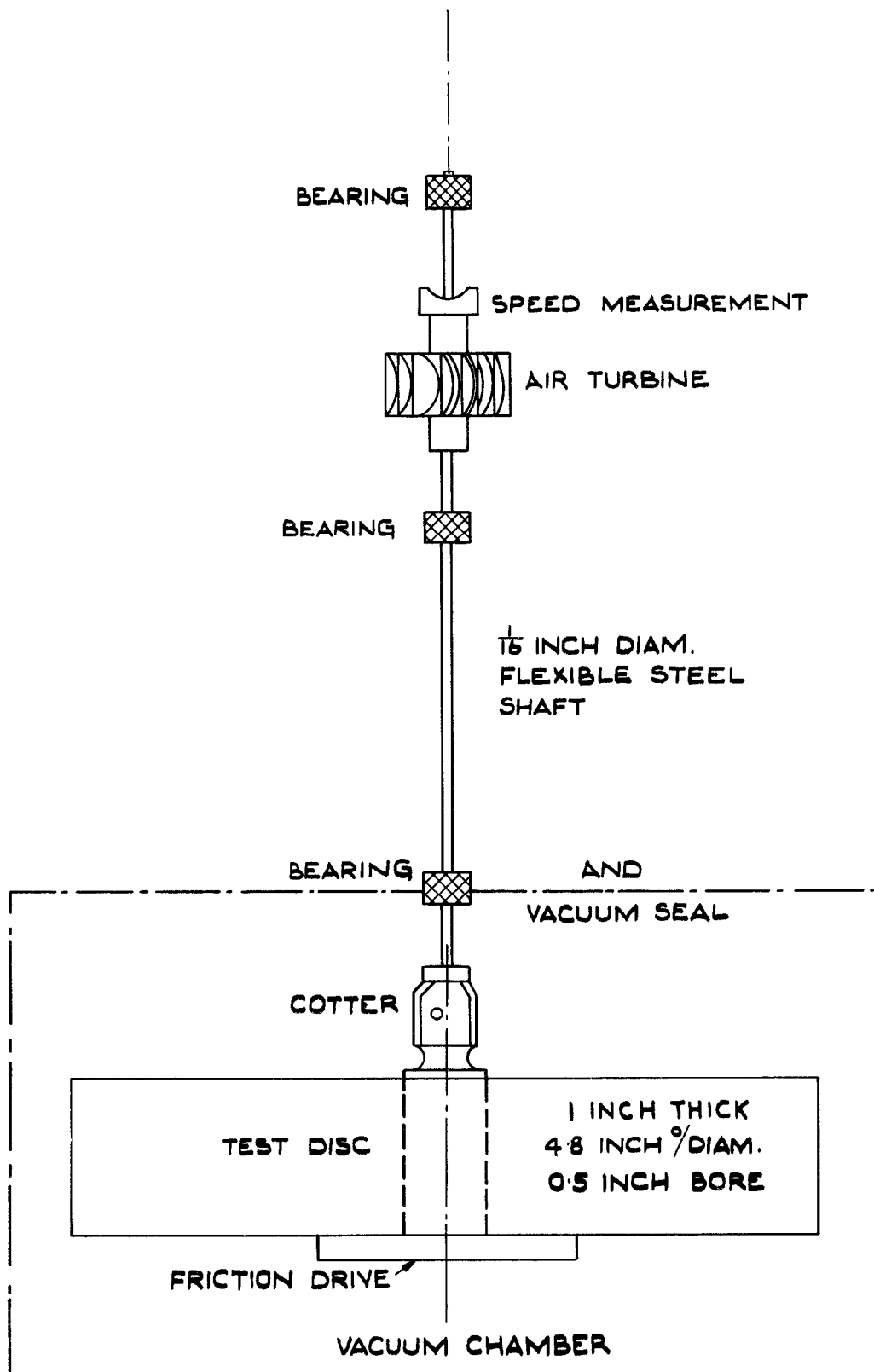
| Reference | Hardness V.P.N. | | Maximum speed rev/min | Nominal average tangential stress tons/sq in. | Maximum thickness at bore inches |
|------------------------------|--------------------|-----|-----------------------------|--|---|
| | Bore | Rim | | | |
| a. <u>Forged/air melt</u> | | | | | |
| 2833 | 447 | 443 | 105,720 | 84.6 | 1.00 |
| 2845 | 446 | 446 | 107,400 | 87.8 | 1.00 |
| 2847 | 444 | 444 | (91,050)* | (62.9) | (0.997) |
| 2834 | 441 | 446 | 50,680 \ddagger | 19.5 | 0.995 |
| 2837 | 432 | 432 | 46,600 \ddagger | 16.5 | 0.995 |
| 2846 | 432 | 430 | 45,540 \ddagger | 15.75 | 0.994 |
| 2840 | 439 | 444 | | Cut for test pieces | |
| 2843 | 473 | 476 | | Spare blank | |
| 2836 | 338 | | (93,960)* | (67.0) | (0.967) |
| 2838 | 336 | | (93,600)* | (66.6) | (0.923) |
| 2839 | 337 | | (92,940) | (65.5) | (0.984) |
| 2841 | 337 | | 56,740 \ddagger | 24.4 | 0.995 |
| 2842 | 339 | | 58,100 \ddagger | 25.6 | 0.995 |
| 2844 | 333 | | 58,620 \ddagger | 26.1 | 0.995 |
| 2835 | 336 | | | Cut for test pieces | |
| b. <u>Forged/vacuum melt</u> | | | | | |
| 2815 | 413 | 415 | 103,200 | 81.2 | 0.920 |
| 2818 | 400 | 406 | 108,600 | 89.5 | 0.946 |
| 2825 | 404 | 402 | (86,400) | (56.6) | (0.998) |
| 2813 | 402 | 404 | 53,520 \ddagger | 21.8 | 0.995 |
| 2821 | 413 | 413 | 46,806 \ddagger | 16.6 | 0.994 |
| 2822 | 409 | 411 | 47,000 \ddagger | 16.75 | 0.993 |
| 2819 | 404 | 409 | | Cut for test pieces | |
| 2826 | 420 | 425 | | Spare blank | |
| 2814 | 308 | | (89,000) | (60.1) | (0.966) |
| 2816 | 331 | | (91,000) | (62.9) | (0.971) |
| 2817 | 308 | | (89,400) | (60.7) | (0.979) |
| 2820 | 305 | | 58,490 \ddagger | 26.0 | 0.994 |
| 2823 | 309 | | 61,940 \ddagger | 29.2 | 0.995 |
| 2824 | 307 | | 63,320 \ddagger | 30.4 | 0.995 |
| 2827 | 306 | | | Cut for test pieces | |

Figures in brackets are for discs not burst

* Cracks

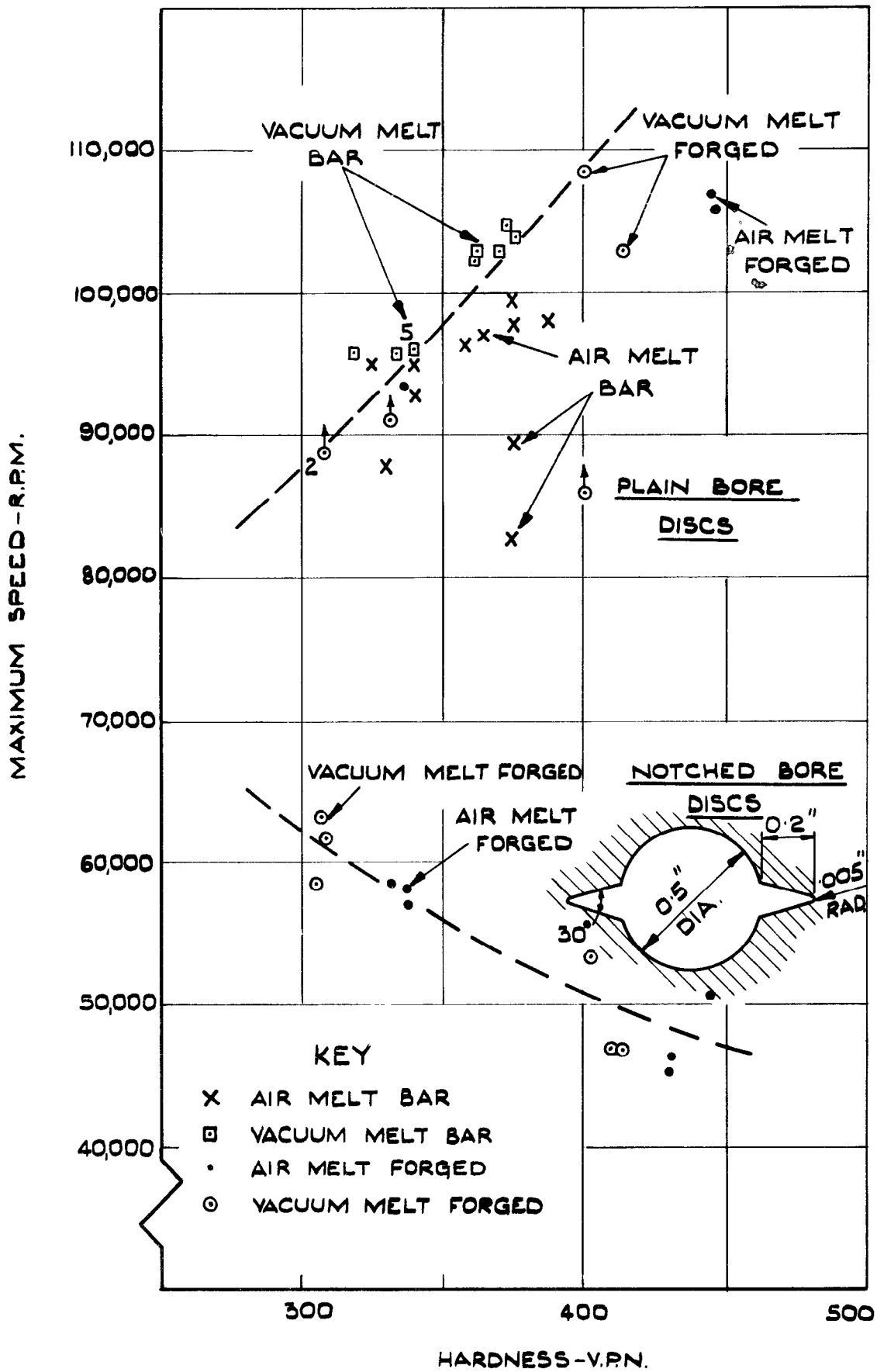
\ddagger Notched bore

FIG. 1



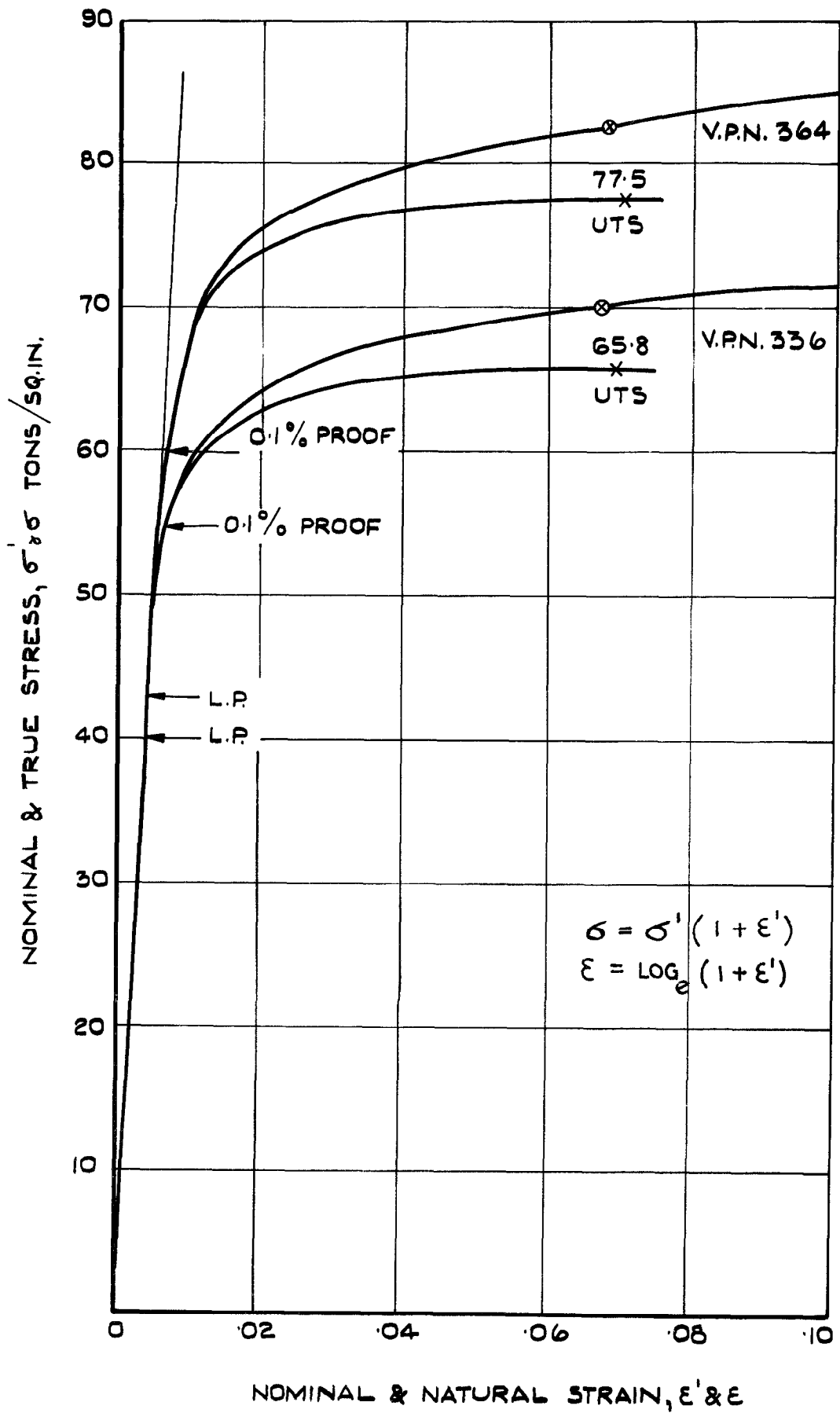
DETAILS OF MODEL DISCS & TEST RIG (FULL SCALE)

FIG. 2

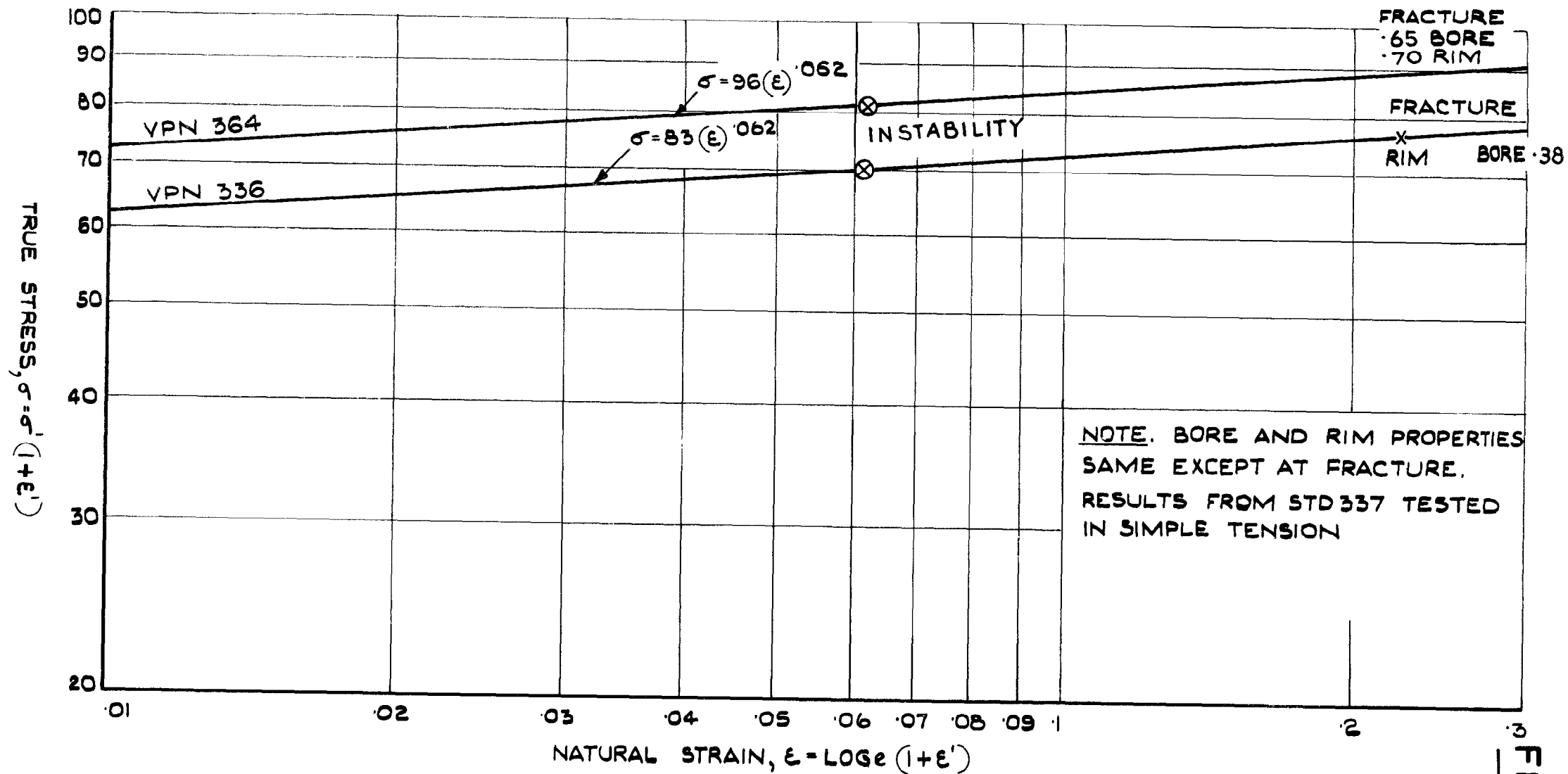


COMPARISON BETWEEN BURST STRENGTH OF AIR & VACUUM MELT (BAR & FORGED) DISCS IN REX 535 STEEL.

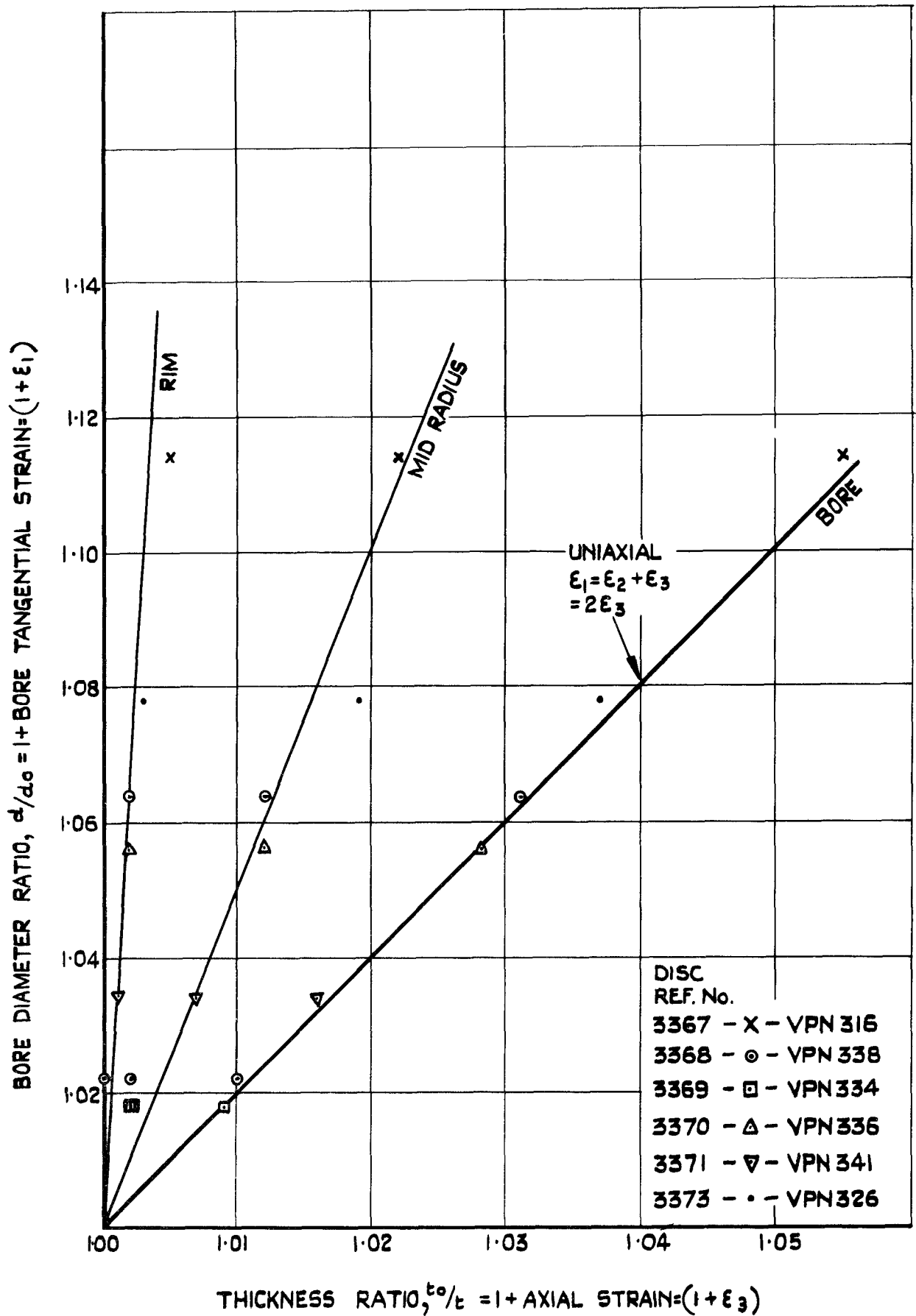
FIG. 3 (a)



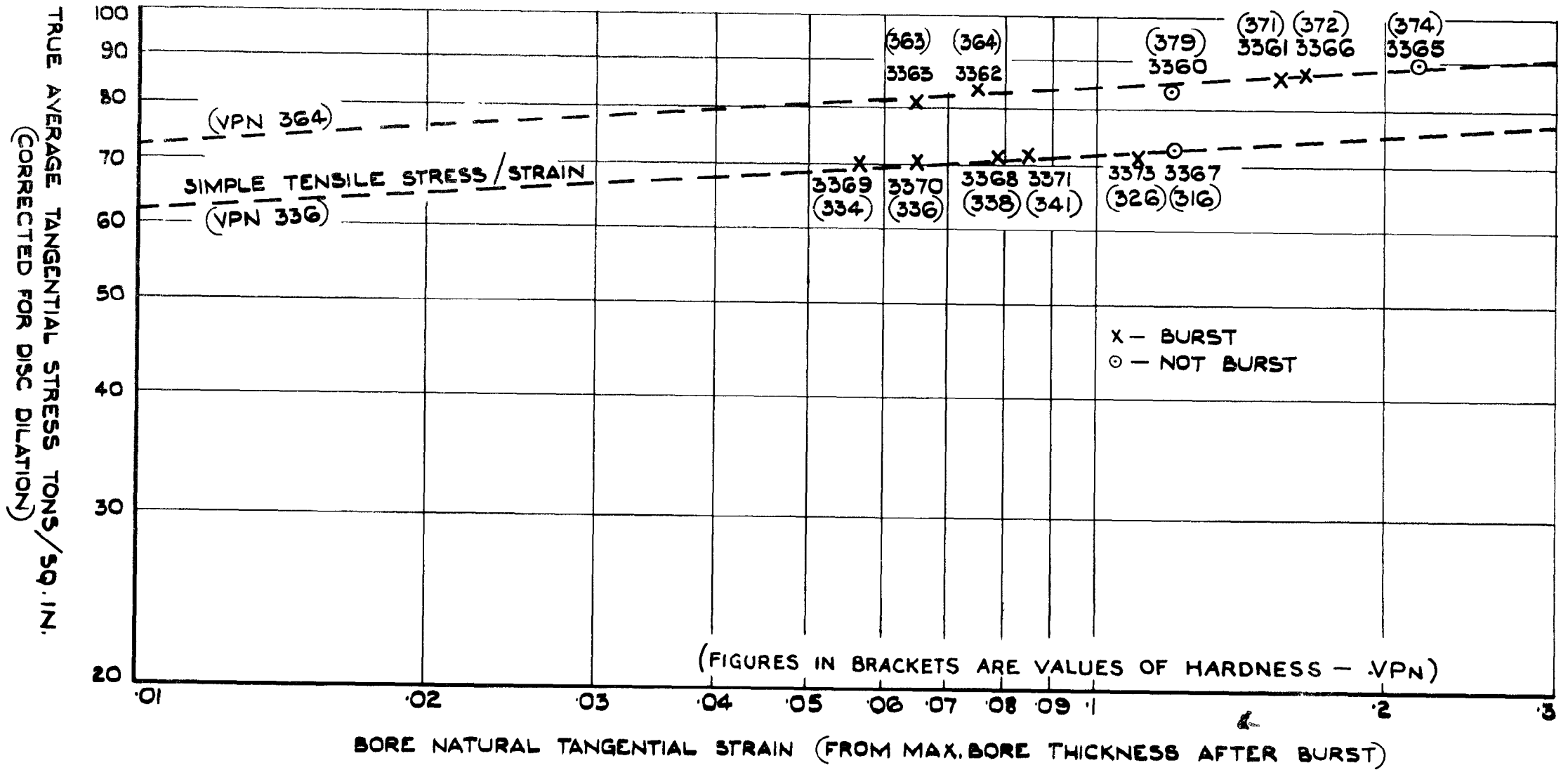
STRESS/STRAIN DATA FOR REX 535 VACUUM MELT BAR.



LOG TRUE STRESS/LOG NAT. STRAIN DATA FOR REX 535 VACUUM MELT BAR.

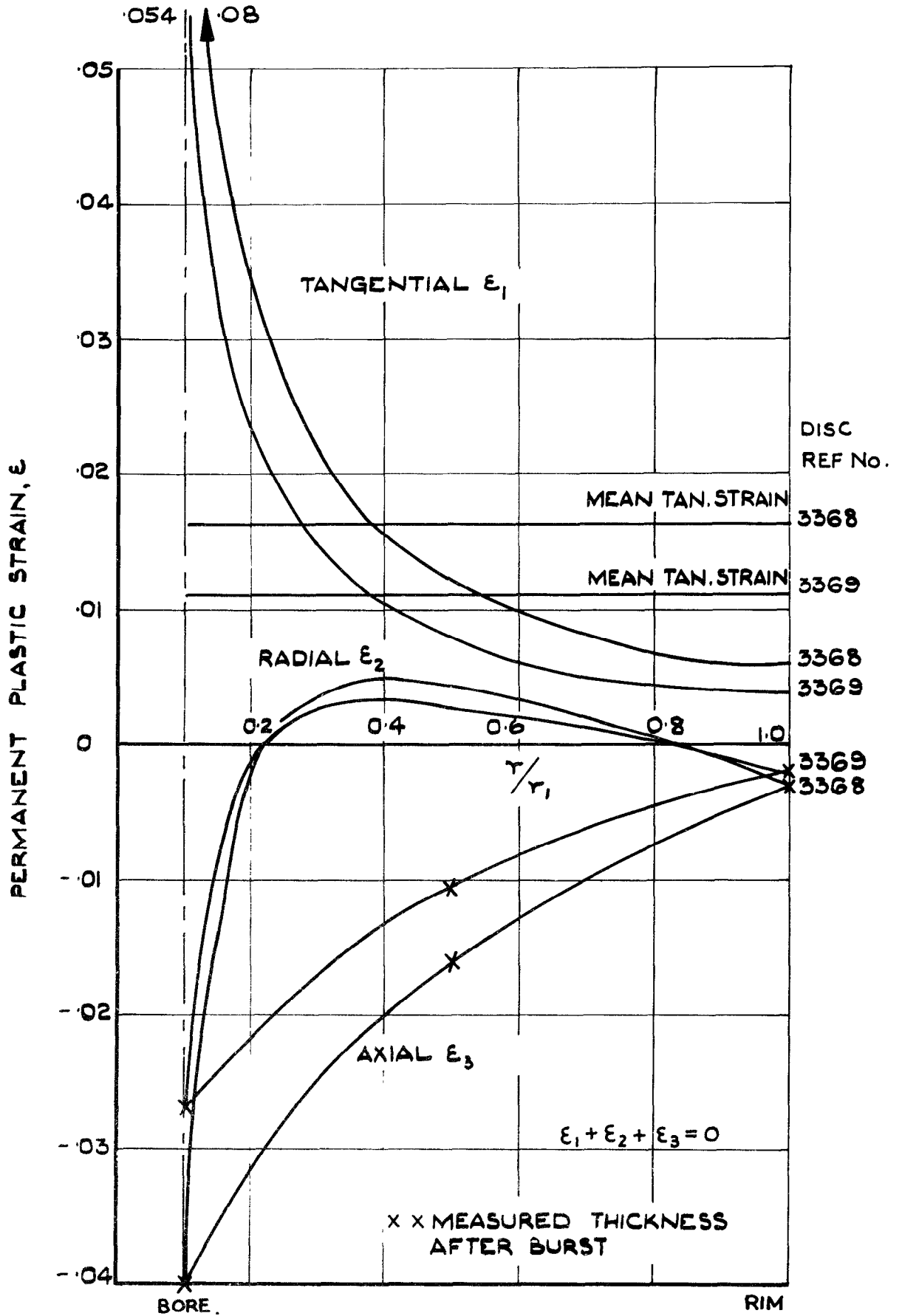


PLASTIC DISTORTION IN DISCS RELATED TO BORE TANGENTIAL STRAIN.



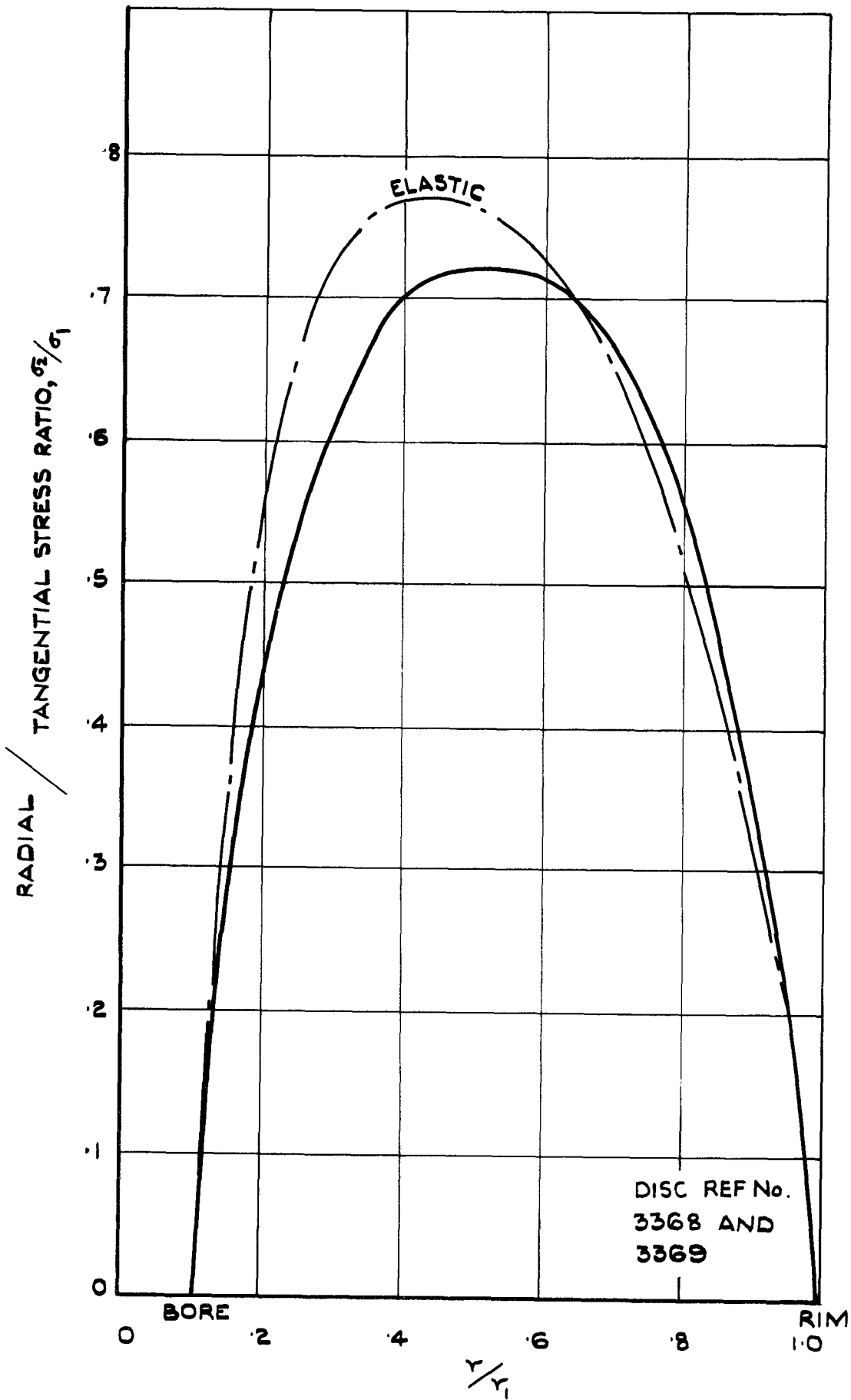
BURST STRENGTH AND DUCTILITY OF DISCS FROM REX 535 VACUUM MELT BAR.

FIG. 6



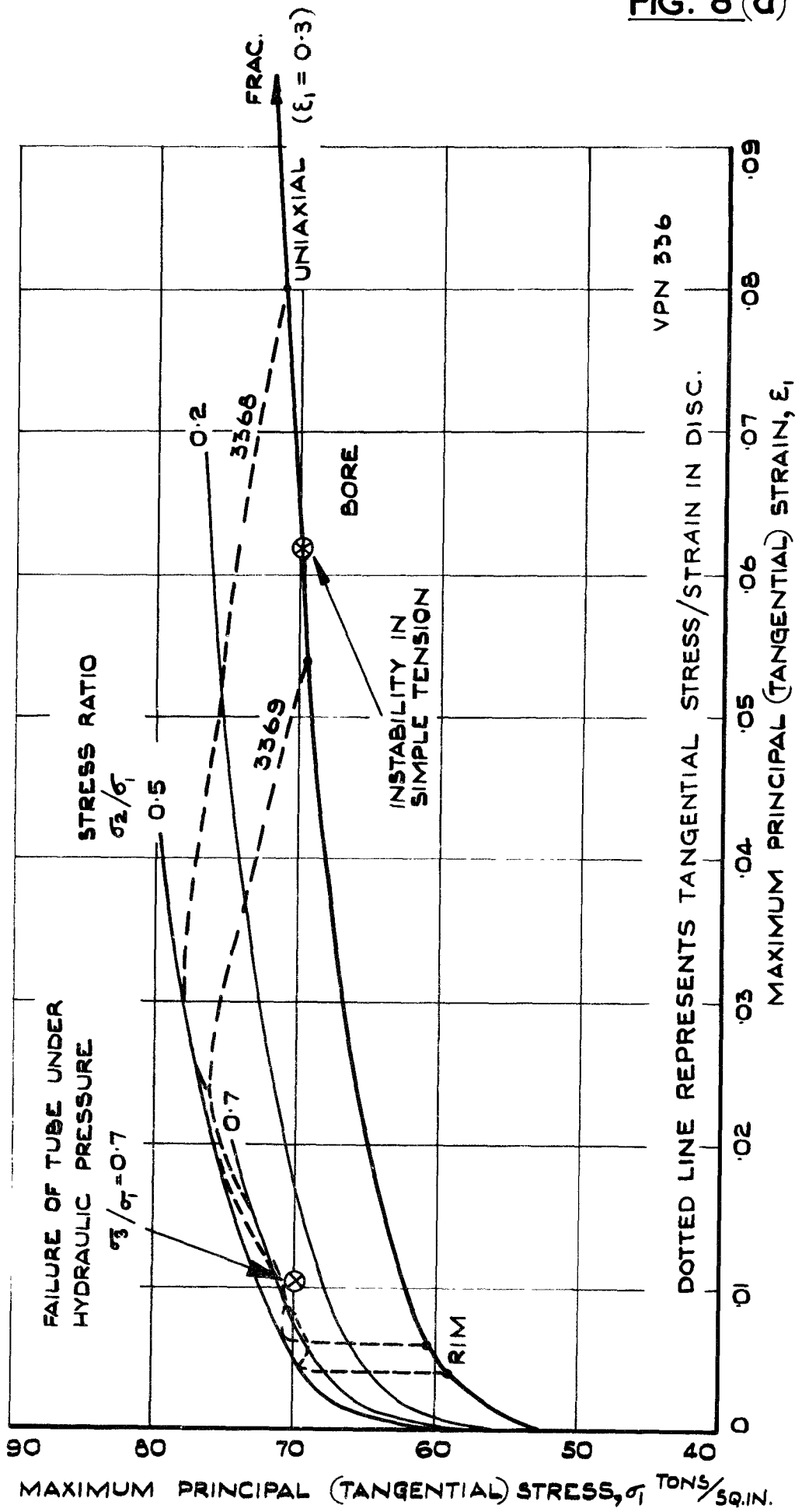
PRINCIPAL PLASTIC STRAINS IN DISC AT BURST.

FIG. 7



DISTRIBUTION OF RADIAL/TANGENTIAL STRESS RATIO
IN DISCS AT BURST.

FIG. 8 (a)



DISTRIBUTION OF TANGENTIAL STRESS/STRAIN
IN DISCS AT BURST. (V.P.N. 336)

**DISTRIBUTION OF TANGENTIAL STRESS/STRAIN IN
DISC AT BURST. (V.P.N. 364)**

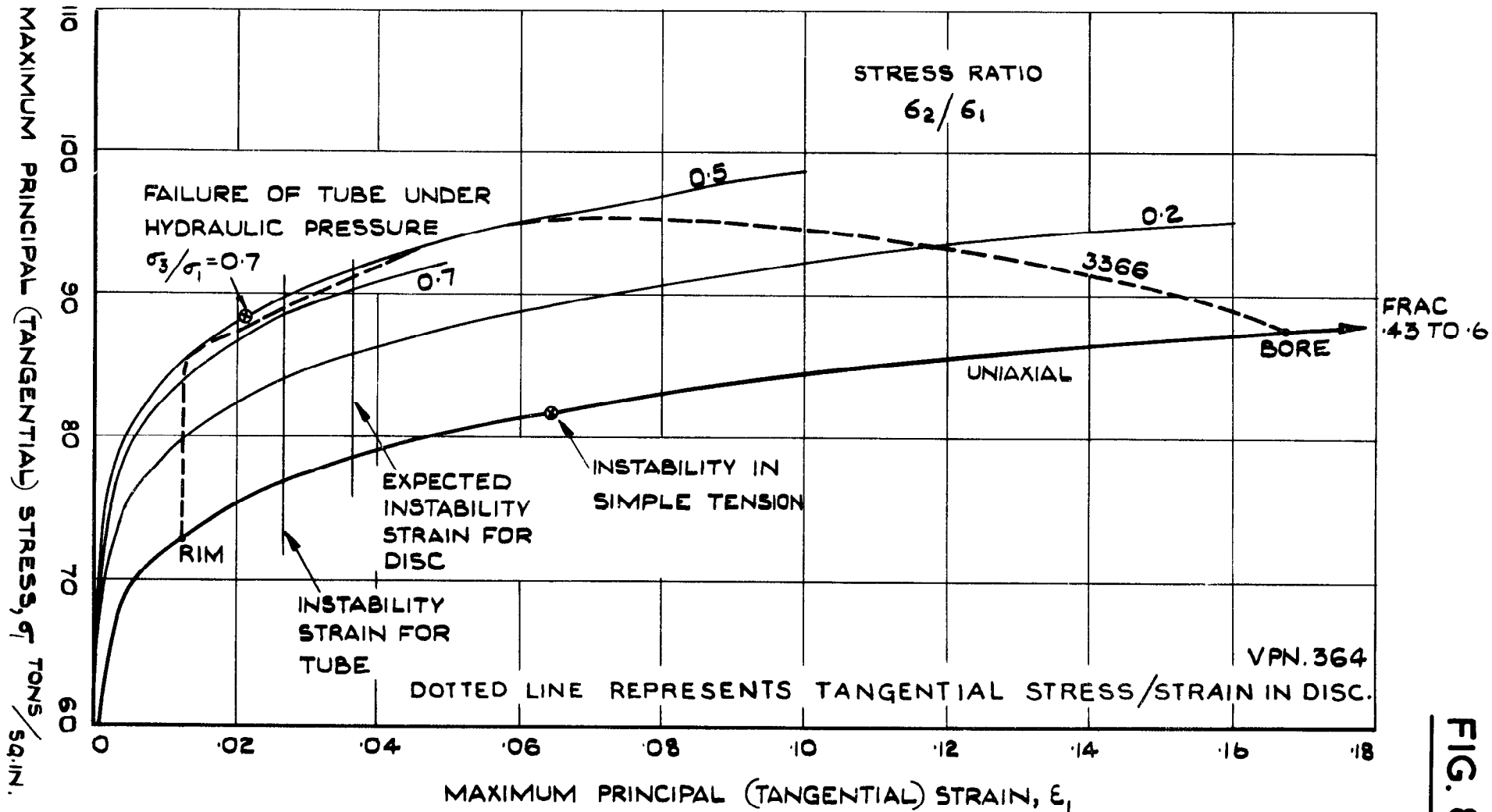
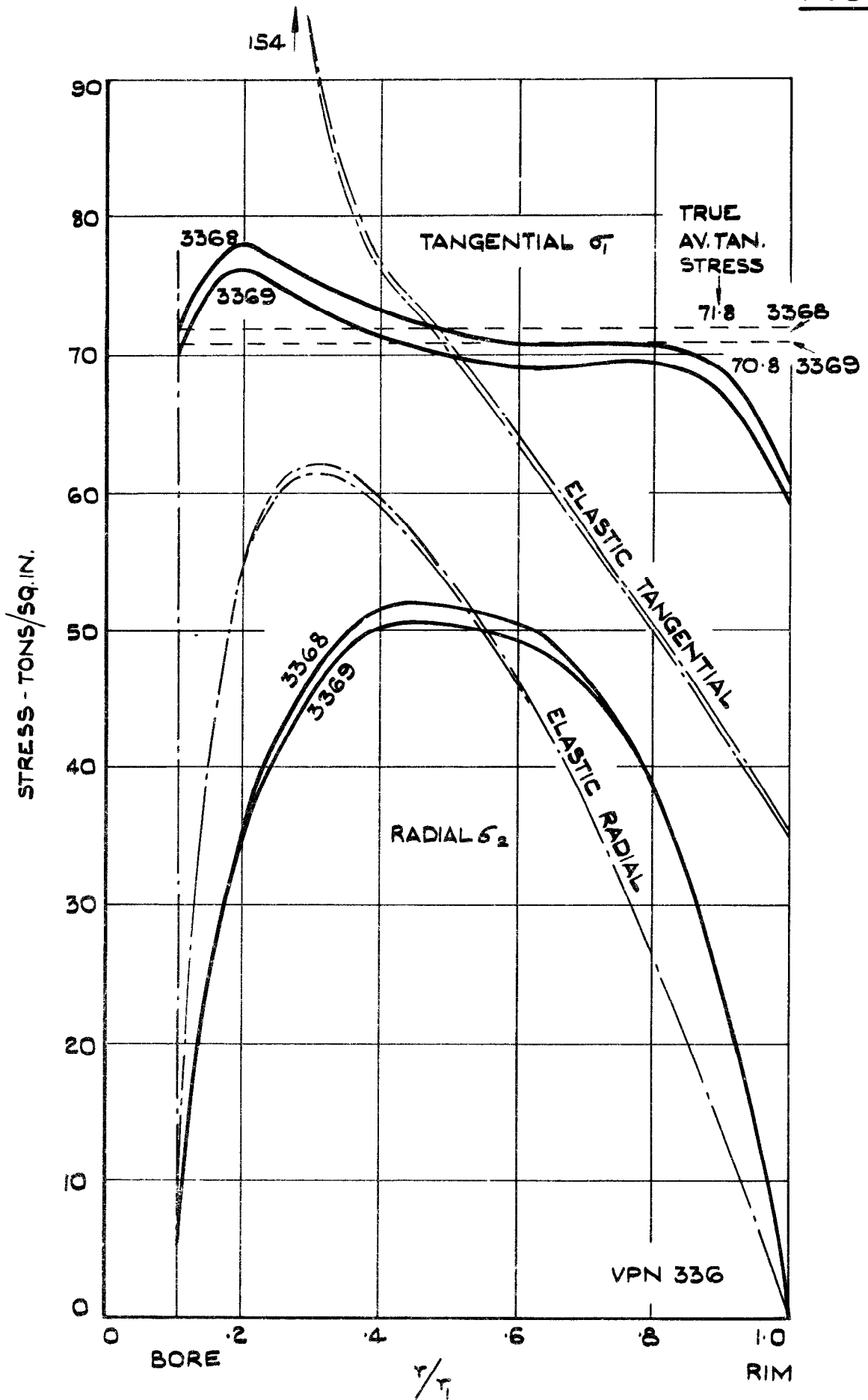


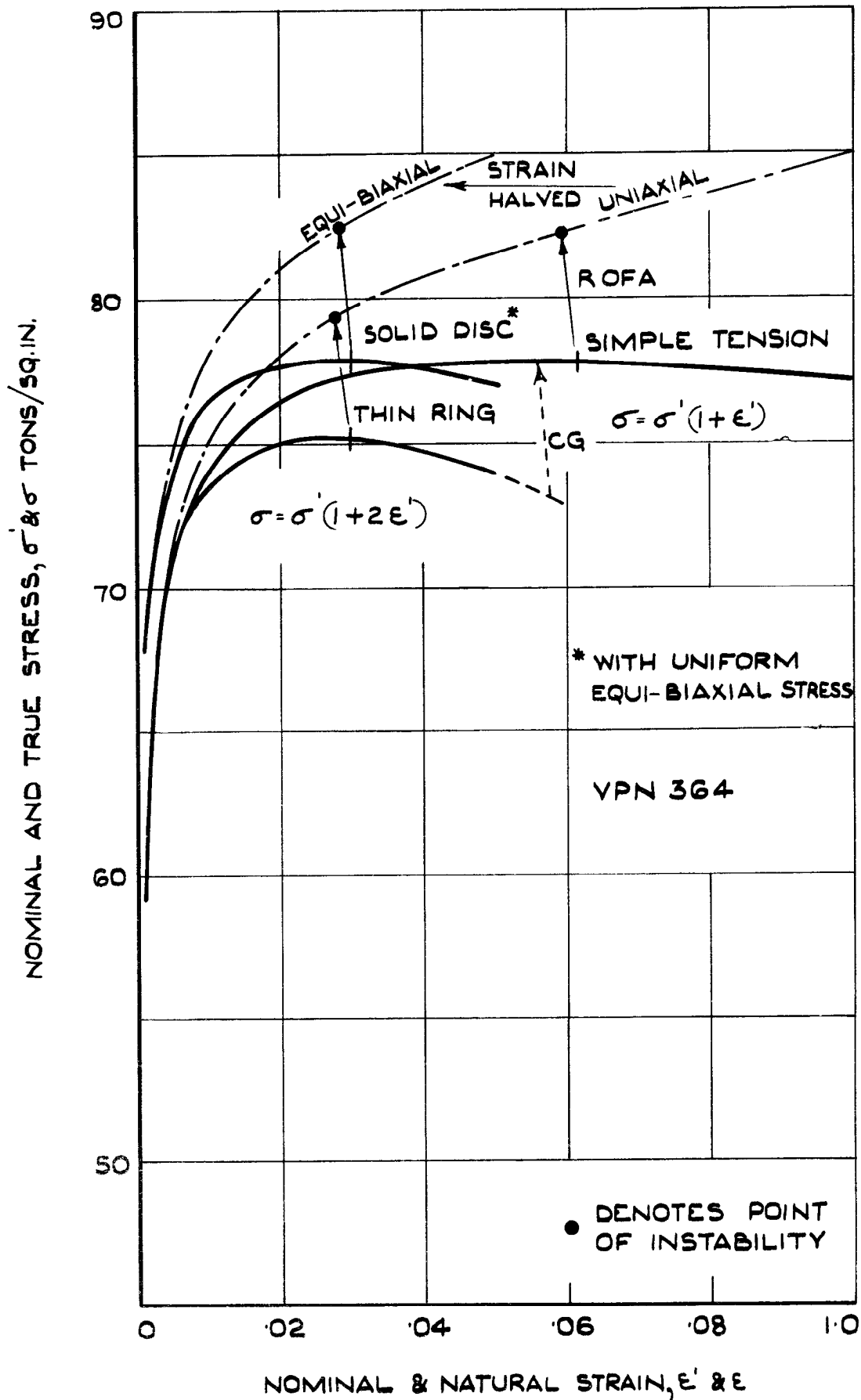
FIG. 8 (b)

FIG. 9

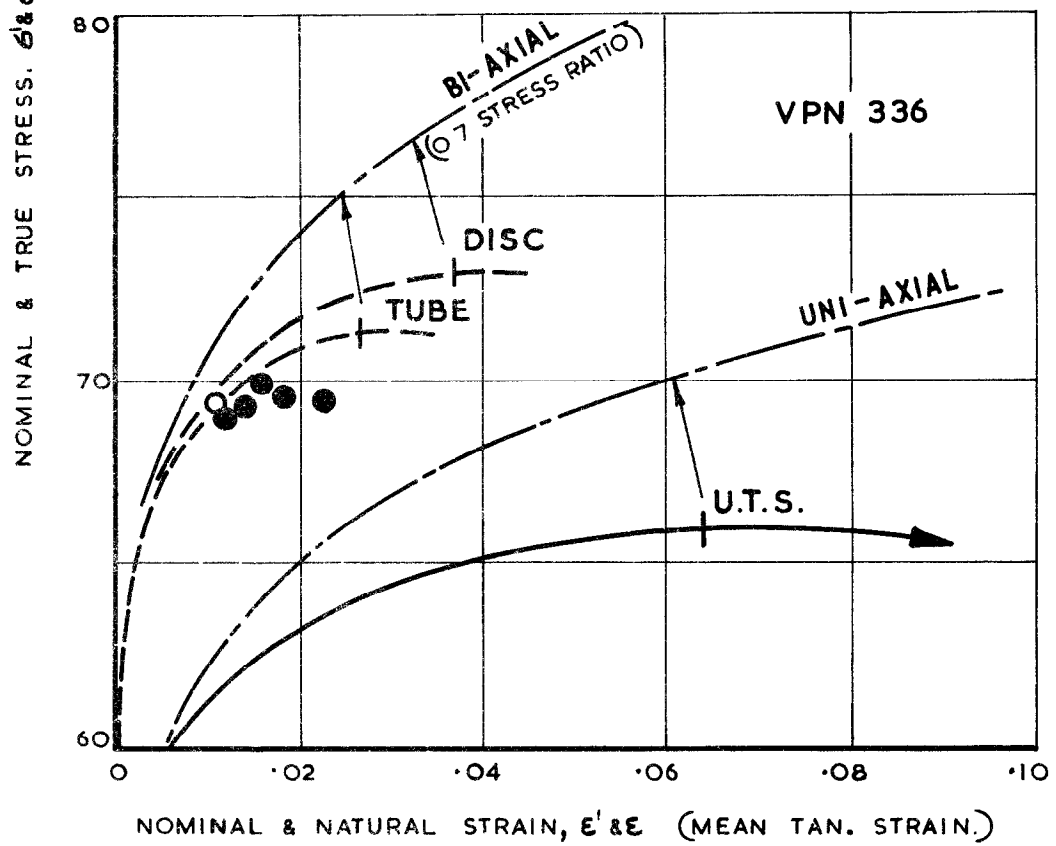
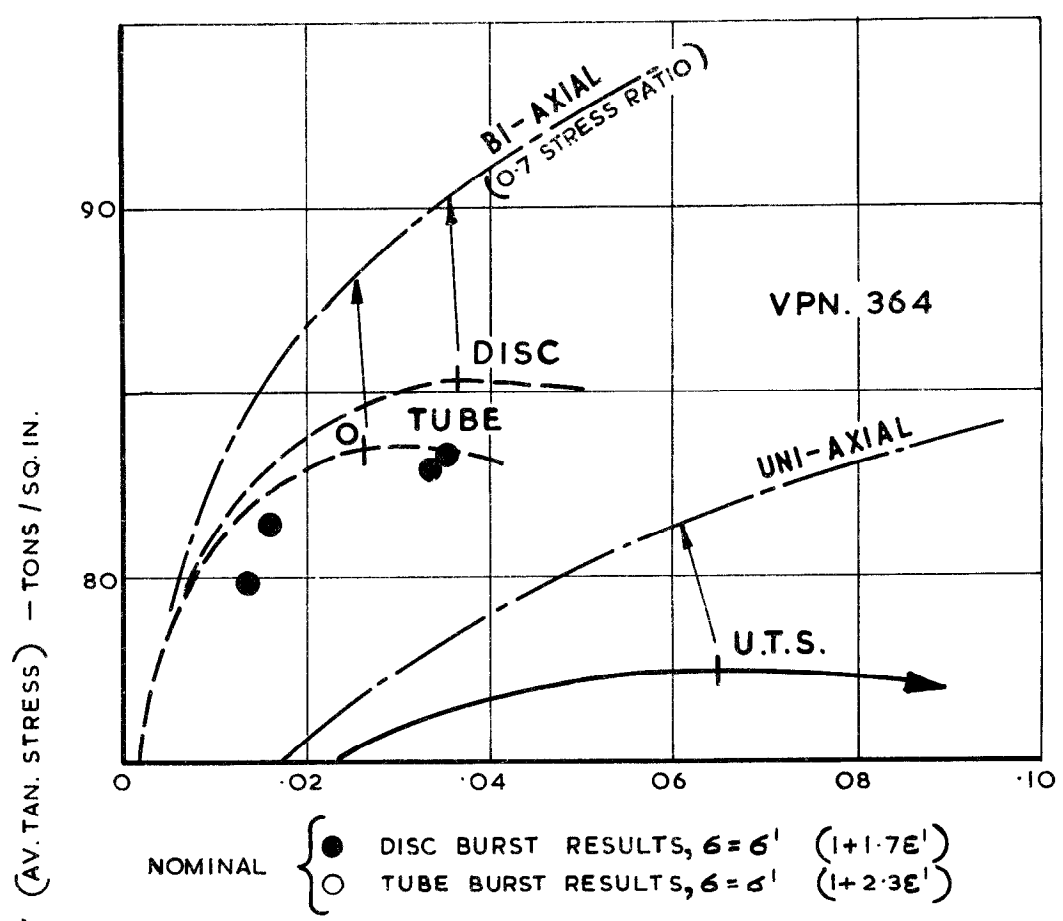


DISTRIBUTION OF STRESS IN DISC AT BURST. (V.P.N. 336)

FIG. 10

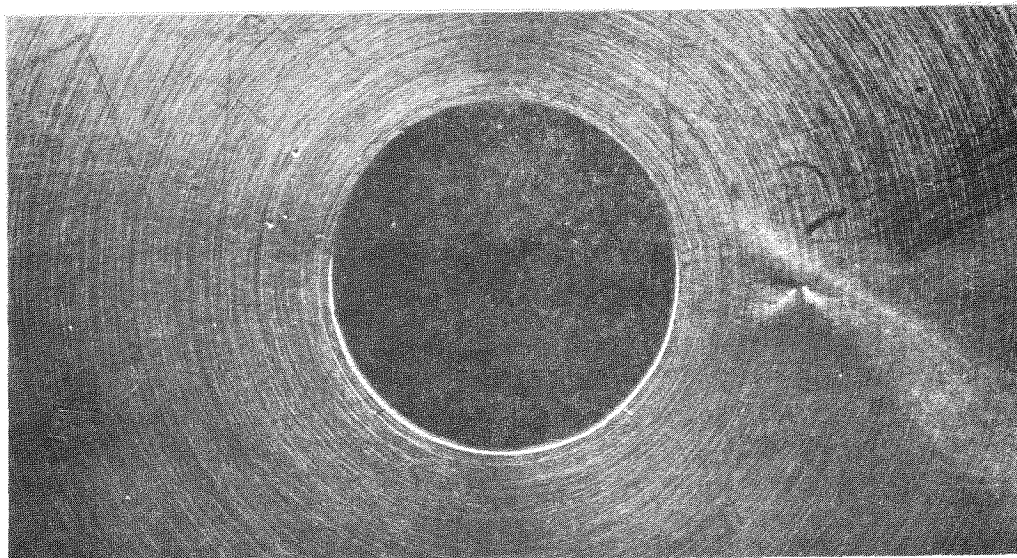


THE INFLUENCE OF GEOMETRY ON INSTABILITY.

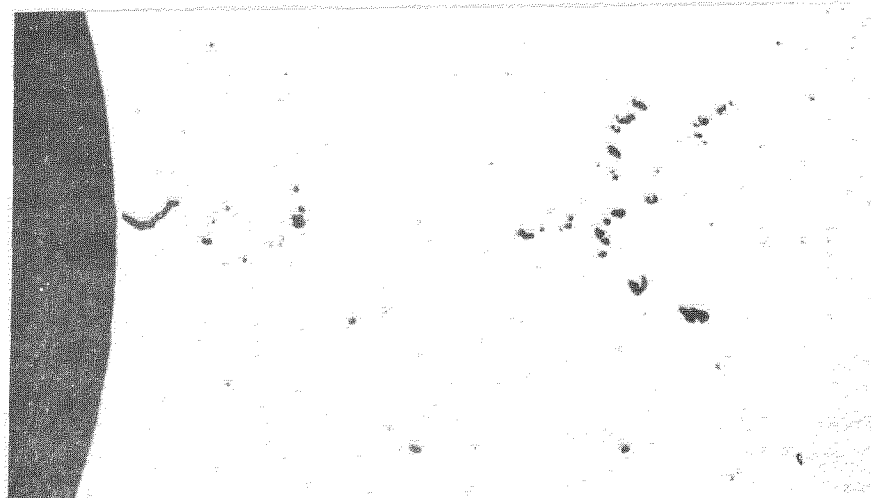


DISC & TUBE NOMINAL BURST RESULTS IN RELATION TO INSTABILITY.

FIG. 2.



SURFACE CRACK NEAR 0.5 DIA. BORE X 4



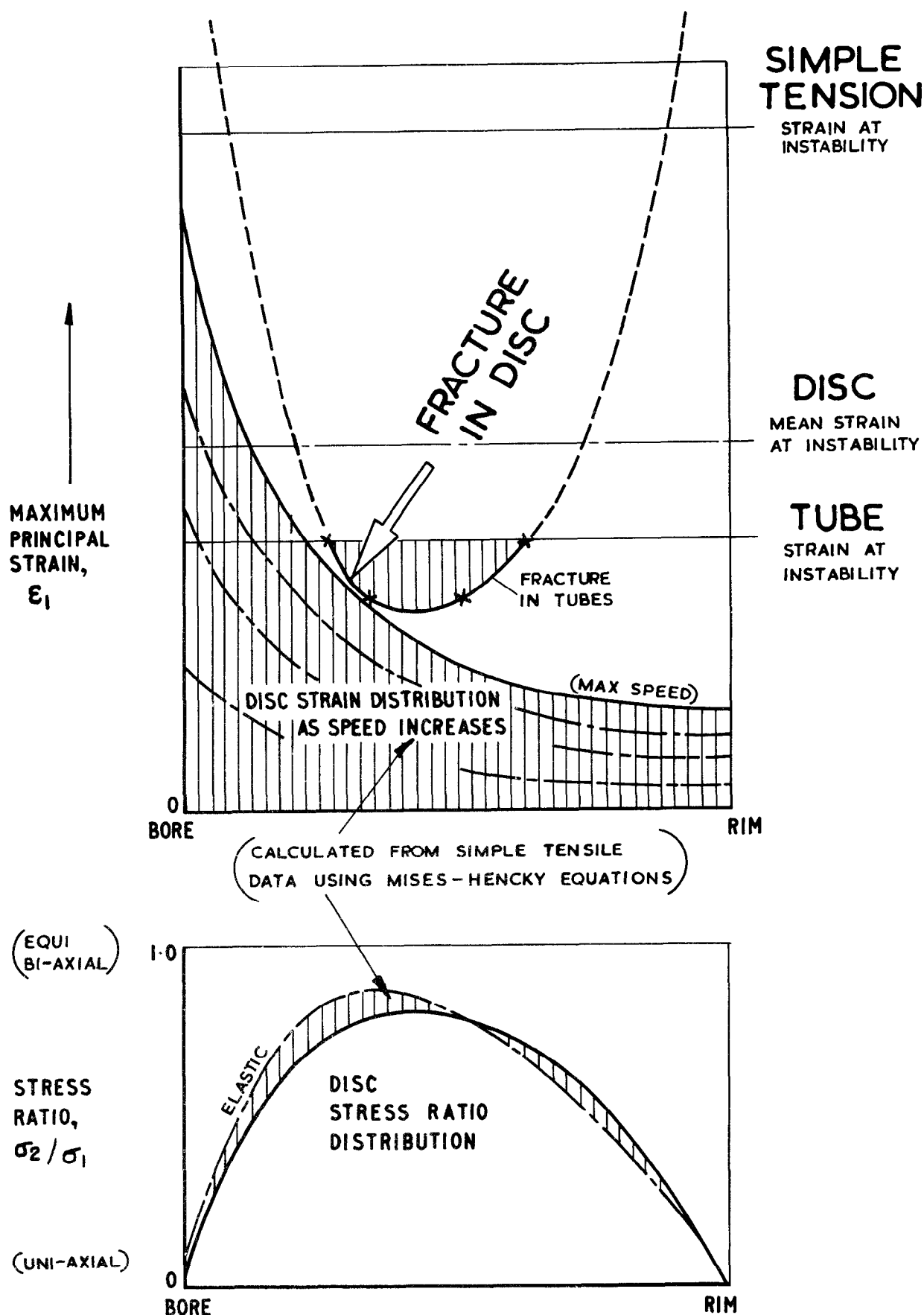
MID AXIAL CRACKS NEAR BORE X 15



MID AXIAL CRACKS NEAR BORE X 50

CRACKS AROUND BORE OF DISC No. 3367 AFTER 12%

FIG. 13



PROPOSED METHOD OF ASSESSING DISC STRENGTH FROM TUBE DATA.

A.R.C. C.P. No. 660 January 1963

531.25-434.3:620.172

Waldren, N. E. and Ward, D. E.

ROOM TEMPERATURE INSTABILITY AND FRACTION
IN ROTATING DISCS AND CORRELATION WITH
BI-AXIAL TENSILE TEST DATA

The room temperature burst strength and ductility of model discs in a typical ferritic turbine disc material (Rex 535) has been examined.

Discs from vacuum melted bar exhibited remarkably consistent properties. The discs burst when the average tangential stress exceeded the ultimate tensile strength of the material by as much as 7 per cent. A detailed analysis of the more ductile discs supports the use of the distortion energy (Von Mises) and deformation (Hencky) theories for predicting disc instability. In the case of the less ductile discs, results from tubes in bi-axial tension confirm failure when this occurs before the point of instability.

A.R.C. C.P. No. 660 January 1963

531.25-434.3:620.172

Waldren, N. E. and Ward, D. E.

ROOM TEMPERATURE INSTABILITY AND FRACTION
IN ROTATING DISCS AND CORRELATION WITH
BI-AXIAL TENSILE TEST DATA

The room temperature burst strength and ductility of model discs in a typical ferritic turbine disc material (Rex 535) has been examined.

Discs from vacuum melted bar exhibited remarkably consistent properties. The discs burst when the average tangential stress exceeded the ultimate tensile strength of the material by as much as 7 per cent. A detailed analysis of the more ductile discs supports the use of the distortion energy (Von Mises) and deformation (Hencky) theories for predicting disc instability. In the case of the less ductile discs, results from tubes in bi-axial tension confirm failure when this occurs before the point of instability.

A.R.C. C.P. No. 660 January 1963

531.25-434.3:620.172

Waldren, N. E. and Ward, D. E.

ROOM TEMPERATURE INSTABILITY AND FRACTION
IN ROTATING DISCS AND CORRELATION WITH
BI-AXIAL TENSILE TEST DATA

The room temperature burst strength and ductility of model discs in a typical ferritic turbine disc material (Rex 535) has been examined.

Discs from vacuum melted bar exhibited remarkably consistent properties. The discs burst when the average tangential stress exceeded the ultimate tensile strength of the material by as much as 7 per cent. A detailed analysis of the more ductile discs supports the use of the distortion energy (Von Mises) and deformation (Hencky) theories for predicting disc instability. In the case of the less ductile discs, results from tubes in bi-axial tension confirm failure when this occurs before the point of instability.

© *Crown copyright* 1963

Printed and published by
HER MAJESTY'S STATIONERY OFFICE

To be purchased from
York House, Kingsway, London w.c.2
423 Oxford Street, London w.1
13A Castle Street, Edinburgh 2
109 St. Mary Street, Cardiff
39 King Street, Manchester 2
50 Fairfax Street, Bristol 1
35 Smallbrook, Ringway, Birmingham 5
80 Chichester Street, Belfast 1
or through any bookseller

Printed in England